Control of a Tubular Chemical Reactor by means of POD and Predictive Control Techniques

Oscar Mauricio Agudelo, Jairo José Espinosa and Bart De Moor

Abstract— **This paper presents the results of applying POD (Proper orthogonal decomposition) and predictive control techniques to the control of a non-isothermal tubular reactor. The control goal is to keep the operation of the reactor around a desired operating condition in spite of the disturbances in the feeding flow. This operating condition is determined by means of an optimization algorithm that provides the optimal temperature and concentration profiles for the system. Around these optimal profiles the nonlinear PDEs (Partial Differential Equations) that model the reactor are linearized, and afterwards the resulting linear PDEs are discretized in space giving as result a high order linear model. Then a reduced order model is found by means of the POD technique which makes possible the design of an MPC controller for rejecting the disturbances that affect the tubular reactor.**

Index Terms — **Tubular Reactors, Proper Orthogonal Decomposition, Model Reduction, Distributed Parameter Systems, Predictive Control.**

I. INTRODUCTION

The dynamics of tubular reactors are typically described by nonlinear PDEs (Partial Differential Equations) which are derived from mass and energy balance principles. The control of such systems can be addressed by transforming the PDEs and the boundary conditions into a set of ODEs (Ordinary Differential Equations), which would make possible the application of the control theory developed for lumped parameter systems. However, the design of the controllers would be very difficult or practically impossible due to the high order models obtained of discretizing the PDEs. Therefore, it is necessary to find reduced-order models that make possible the design of the control schemes. In this paper such reduced-order models are derived by means of Proper Orthogonal Decomposition (POD) and Galerkin projection.

Proper Orthogonal Decomposition is a technique that has been applied in many physical systems governed by PDEs for deriving reduced order models. The advantage of applying this technique is the incorporation of simulation or experimental data as well as the existing physical relationships (when the Galerkin projection is used) from the original model [6].

This paper presents the application of POD and Predictive control techniques to the control of the temperature and concentration profiles of a non-isothermal tubular reactor. An MPC controller was designed for rejecting the disturbances that affect the tubular reactor, that is the changes in the temperature and concentration of the feeding flow. This MPC is based on the reduced order model of the process which was derived by means of the POD technique.

Additionally in this paper, an optimization algorithm is proposed for deriving the optimal operating profiles of the tubular reactor.

This paper presents a description of the process in section II. Also in this section the optimization algorithm for obtaining the optimal operating profiles is discussed. Section III shows the derivation of the reduced order model of the reactor by means of POD. In section IV the design of the MPC controller is described. Besides the simulation results are presented. Finally section V draws the main conclusions.

II. TUBULAR CHEMICAL REACTOR

The system to be controlled is a non-isothermal tubular reactor where a single, first order, irreversible, exothermic reaction takes place ($A \rightarrow B$). The reactor is surrounded by 3 cooling/heating jackets as it is shown in figure 1. The temperature of the jackets fluids (T_{J1}, T_{J2} and T_{J3}) can be manipulated independently in order to control the concentration and temperature profiles inside the reactor. In this study the heat transfer effects between the jackets fluids and the reactor wall are neglected. Therefore the temperature of the jacket fluids would be equivalent to the temperature of the reactor wall. Additionally, a plug-flow behavior inside the reactor is assumed, which means that the diffusion and dispersion phenomena are not taken into account. Under the previous assumptions, the mathematical model of the tubular chemical reactor consists of the following coupled non-linear PDEs:

$$\begin{aligned} \frac{\partial C}{\partial t} &= -v\frac{\partial C}{\partial z} - k_0 C e^{-\frac{E}{RT}} \\ \frac{\partial T}{\partial t} &= -v\frac{\partial T}{\partial z} + G_r C e^{-\frac{E}{RT}} + H_r(T_w - T) \qquad (1) \\ G_r &= \frac{-\Delta H k_0}{\rho C_p}, \quad H_r = \frac{4h}{d\rho C_p} \end{aligned}$$

with the following boundary conditions (tubular reactor with closed ends):

$$C = C_{in} \text{ at } z = 0 \text{ and } T = T_{in} \text{ at } z = 0$$

O. M. Agudelo is with the Department of Electrical Engineering (ESAT), Research Group SCD-SISTA, Katholieke Universiteit Leuven, Kasteelpark Arenberg 10, B-3001 Heverlee (Leuven), Belgium. He is also with the Department of Automation and Electronics, Universidad Autónoma de Occidente, Calle 25 No 115-85, Cali, Colombia. mauricio.agudelo@esat.kuleuven.be

J. J. Espinosa is with the Facultad de Minas, Universidad Nacional de Colombia, Carrera 80 No. 65-223, Medellin, Colombia. jairo.espinosa@ieee.org

B. De Moor is with the Department of Electrical Engineering (ESAT), Research Group SCD, Katholieke Universiteit Leuven, Kasteelpark Arenberg 10, B-3001 Heverlee (Leuven), Belgium. bart.demoor@esat.kuleuven.be

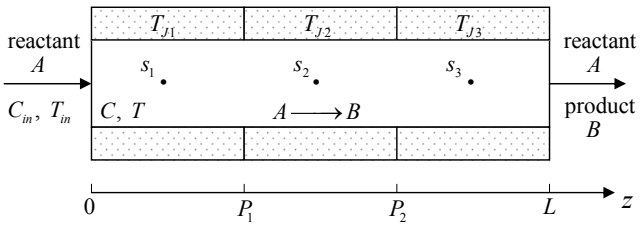

Fig. 1. Tubular Chemical Reactor with 3 cooling/heating jackets.

TABLE I
VALUES OF THE REACTOR PARAMETERS

$v = 0.1$ m·s^{-1}
$L = 1$ m
$k_0 = 10^6$ s^{-1}
$E = 11250$ cal·mole^{-1}
$R = 1.986$ cal·mole^{-1}·K^{-1}
$C_{in} = 0.02$ mole·L^{-1}
$T_{in} = 340$ K
$G_r = 4.25 \cdot 10^9$ L·K·mole^{-1}·s^{-1}
$H_r = 0.2$ s^{-1}

where $C(z,t)$ is the reactant concentration in [mole/L], $T(z,t)$ is the reactant temperature in [K], v is the fluid superficial velocity in [m/s], $(-\Delta H)$ is the heat of the reaction in [cal/mole], ρ and C_p are the density in [Kg/L] and the specific heat in [cal/Kg/K] respectively, k_0 is the kinetic constant in [1/s], E is the activation energy in [cal/mole], R is the ideal gas constant in [cal/mole/K], h is the heat transfer coefficient in [cal/s/m^2/K], d is the reactor diameter in [m], L is the reactor length in [m], C_{in} and T_{in} are the concentration in [mole/L] and the temperature in [K] of the feeding flow, z is the axial coordinate in [m], t is the time in [s] and $T_w(z,t)$ is the reactor wall temperature in [K] defined as follows (see figure 1),

$$T_w = \begin{cases} T_{J1}, & 0 \le z < P_1 \\ T_{J2}, & P_1 \le z < P_2 \\ T_{J3}, & P_2 \le z \le L. \end{cases}$$

The parameters values of the reactor model are taken from [1] which were inspired by the values given in [2]. These values are presented in table I.

The temperature of the jacket sections T_{J1}, T_{J2} and T_{J3} must be between 280 K and 400 K (input constraints). In addition, the temperature inside the reactor must be smaller than 400 K (state constraint) in order to avoid the formation of side products. The kind of disturbances that affects the reactor are the variations in the temperature and concentration of the feeding flow. Typically such variations are ± 10 K for temperature and $\pm 5\%$ of the nominal value for the concentration. In this system only the temperature of the feeding flow is measured directly. In addition, the reactor has a temperature sensor at the output and 3 temperature sensors (s_1, s_2 and s_3) distributed in its interior as it is shown in figure 1.

A. Operating Point

The steady-state concentration and temperature profiles of the reactor were found by means of an optimization algorithm, which minimizes a cost function subjected to the steady-state equations of the tubular chemical reactor described by (1) and the input and state constraints defined previously. This steady-state model is given by the following ODEs (Ordinary Differential Equations):

$$\begin{aligned} \frac{dC}{dz} &= -\frac{k_0}{v} C e^{-\frac{E}{RT}} \\ \frac{dT}{dz} &= \frac{G_r}{v} C e^{-\frac{E}{RT}} + \frac{H_r}{v}(T_w - T) \end{aligned} \quad (2)$$

with $T = T_{in}$ at $z = 0$ and $C = C_{in}$ at $z = 0$. A discrete version of (2) can be derived by replacing the spatial derivatives by forward difference approximations as follows:

$$\begin{aligned} \bar{C}_{i+1} &= \bar{C}_i - \frac{k_0 \Delta z}{v} \bar{C}_i e^{\frac{-E}{RT_f \bar{T}_i}} \\ \bar{T}_{i+1} &= \bar{T}_i \left[1 - \frac{H_r \Delta z}{v}\right] + \\ &+ \left[\frac{G_r \Delta z C_f}{v T_f}\right] \bar{C}_i e^{\frac{-E}{RT_f \bar{T}_i}} + \left[\frac{H_r \Delta z}{v}\right] \bar{T}_{w,i} \\ \bar{T}_0 &= \frac{T_{in}}{T_f}, \bar{C}_0 = \frac{C_{in}}{C_f} \\ & for\ i = 1, 2, .., N \end{aligned} \quad (3)$$

where $\bar{C}_i = C_i/C_f$ and $\bar{T}_i = T_i/T_f$ are the normalized concentration and temperature of the i-th section, $\bar{T}_{w,i} = T_{w,i}/T_f$ is the normalized temperature of the reactor wall of the i-th section, N is the number of sections in which the reactor is divided, T_f and C_f are normalization factors, and Δz is the length of each section. The variables are normalized in order to avoid possible numerical problems.

The minimization problem that is solved by the optimization algorithm is defined as:

$$\min_{\bar{T}_{J1}, \bar{T}_{J2}, \bar{T}_{J3}} w(\bar{C}_r - \bar{C}_N)^2 + (1-w)\frac{1}{N}\sum_{i=1}^{N}\left(\bar{T}_{r,i} - \bar{T}_i\right)^2 \quad (4)$$

subject to

$$\begin{aligned} &\text{steady} - \text{state model given by (3)} \\ &\frac{T_{\text{jmin}}}{T_f} \le \bar{T}_{J1}, \bar{T}_{J2}, \bar{T}_{J3} \le \frac{T_{\text{jmax}}}{T_f} \\ &\bar{T}_i \le \frac{T_{\max}}{T_f}\ , \quad for\ i = 1, 2, .., N \end{aligned}$$

where $\bar{C}_r$ is the desired concentration (normalized) at the reactor output, $\bar{T}_{r,i}$ is the desired temperature (normalized) inside the reactor of the i-th section, $\bar{C}_N$ is the concentration (normalized) at the reactor output, w is a trade-off coefficient, T_{jmin} and T_{jmax} are the lower and upper temperature values of the fluids of the jackets, and $T_{\max}$ is the maximum allowed temperature inside the tubular reactor.

The first term of the cost function corresponds to the squared error of the normalized concentration at the reactor output (terminal cost), and the second term is related to the

mean squared error of the normalized temperature along the reactor (integral cost). In this problem $\bar{C}_r$ was set to 0, and $\bar{T}_{r,i}$ was selected equal to the normalized temperature of the feeding flow ($\bar{T}_{in} = \frac{T_{in}}{T_f}$) for $i = 1, 2, ..., N$. The trade-off parameter w can take values from 0 to 1. When w goes to 1, the reduction of the reactant concentration at the reactor output becomes more important than the temperature deviations. On the other hand when w goes to 0, the temperature deviations become more important than the concentration at the reactor output and the risk of the formation of hot spots is reduced.

In order to solve the optimization problem described by (4) the following algorithm was proposed:

1) Choose the initial values of the jackets temperatures ($\bar{\mathbf{T}}_J^* = (\bar{T}_{J1}^*, \bar{T}_{J2}^*, \bar{T}_{J3}^*)^T$) in such a way that the constraints are satisfied.
2) Using $\bar{\mathbf{T}}_J^*$, simulate (3) in order to obtain the temperature ($\bar{\mathbf{T}}^* \in \Re^N$) and concentration ($\bar{\mathbf{C}}^* \in \Re^N$) profiles of the reactor in steady state.
3) Linearize the nonlinear model given by (3) around $\bar{\mathbf{T}}^*$,$\bar{\mathbf{C}}^*$, and $\bar{\mathbf{T}}_J^*$ by means of the Taylor series. The resulting linear model would have the following structure:

$$\begin{pmatrix} \bar{C}_{i+1}^{\Delta} \\ \bar{T}_{i+1}^{\Delta} \end{pmatrix} = \mathbf{A}_{ss}(i) \begin{pmatrix} \bar{C}_i^{\Delta} \\ \bar{T}_i^{\Delta} \end{pmatrix} + \mathbf{B}_{ss} \bar{T}_{w,i}^{\Delta} \quad (5)$$

$$\begin{pmatrix} \bar{C}_i \\ \bar{T}_i \end{pmatrix} = \begin{pmatrix} \bar{C}_i^{\Delta} \\ \bar{T}_i^{\Delta} \end{pmatrix} + \begin{pmatrix} \bar{C}_i^{*} \\ \bar{T}_i^{*} \end{pmatrix}$$

$$for\ i = 1, 2, .., N$$

where $\mathbf{A}_{ss}(i)$ and $\mathbf{B}_{ss}$ are the matrices describing the system dynamics, $\bar{C}_i^*$, $\bar{T}_i^*$ and $\bar{T}_{w,i}^*$ are the normalized operating points of the concentration, temperature and reactor wall temperature of the i-th section, $\bar{C}_i^{\Delta}$, $\bar{T}_i^{\Delta}$ and $\bar{T}_{w,i}^{\Delta}$ are the normalized deviation variables of the concentration, temperature and reactor wall temperature respectively.

4) Solve the following Quadratic Problem (QP):

$$\min_{\bar{T}_{J1}^{\Delta}, \bar{T}_{J2}^{\Delta}, \bar{T}_{J3}^{\Delta}} w(\bar{C}_r - \bar{C}_N)^2 + (1-w)\frac{1}{N}\sum_{i=1}^{N}\left(\bar{T}_{r,i} - \bar{T}_i\right)^2$$

subject to

$$\text{steady} - \text{state linear model given by (5)}$$

$$\frac{T_{\text{jmin}}}{T_f} \leq \bar{T}_{J1}, \bar{T}_{J2}, \bar{T}_{J3} \leq \frac{T_{\text{jmax}}}{T_f}$$

$$\frac{-T_J^{\Delta_{max}}}{T_f} \leq \bar{T}_{J1}^{\Delta}, \bar{T}_{J2}^{\Delta}, \bar{T}_{J3}^{\Delta} \leq \frac{T_J^{\Delta_{max}}}{T_f}$$

where $\bar{T}_{J1}^{\Delta}, \bar{T}_{J2}^{\Delta}, \bar{T}_{J3}^{\Delta}$ are the normalized deviation variables of the jackets temperatures, and $T_J^{\Delta_{max}}$ is a "Local input constraint" which limits the range of the jackets temperatures in such a way that the linear model still approximates the non-linear model. If the linear model does not approximate well the nonlinear model, then we would have convergence problems.

TABLE II

RESULTS OBTAINED WITH THE OPTIMIZATION ALGORITHM

Initial Jackets Temperatures			Final Jackets Temperatures			Number of iterations
T_{J1}	T_{J2}	T_{J3}	T_{J1}	T_{J2}	T_{J3}	
- First Minimum -						
300	300	300	359.6	348.5	291.5	66
350	350	350	359.6	348.5	291.5	73
280	400	280	359.6	348.5	291.5	91
- Second Minimum -						
350	280	350	374.6	310.1	325.2	38
370	290	370	374.6	310.1	325.2	39
- Third Minimum -						
280	280	400	340.7	355.1	365.7	29
380	340	400	340.7	355.1	365.7	24

5) Calculate the new jackets temperatures $\bar{\mathbf{T}}_J^{op} \in \Re^3$ as follows:

$$\bar{\mathbf{T}}_J^{op} = \bar{\mathbf{T}}_J^{\Delta,op} + \bar{\mathbf{T}}_J^*$$

where $\bar{\mathbf{T}}_J^{\Delta,op}$ is the solution of the QP problem stated in the previous step.
6) Using $\bar{\mathbf{T}}_J^{op}$, simulate (3) in order to obtain the new temperature ($\bar{\mathbf{T}}^{op} \in \Re^N$) and concentration ($\bar{\mathbf{C}}^{op} \in \Re^N$) profiles of the reactor in steady state.
7) If $\max\left(\left|\bar{\mathbf{T}}_J^{op} - \bar{\mathbf{T}}_J^*\right|\right) \leq Tol$ then stop, else make $\bar{\mathbf{T}}_J^* = \bar{\mathbf{T}}_J^{op}$, $\bar{\mathbf{C}}^* = \bar{\mathbf{C}}^{op}$, $\bar{\mathbf{T}}^* = \bar{\mathbf{T}}^{op}$ and go to step 3.

The proposed algorithm was executed with the following parameters : $N = 300$, $T_f = 80$ K, $C_f = 0.02$ mole/L, $\Delta z = 1/300$ m, $T_{\text{jmin}} = 280$ K, $T_{\text{jmax}} = 400$ K, $T_{\max} = 390$ K, $Tol = 10^{-4}$, $w = 0.3$ and $T_J^{\Delta_{max}} = 20$ K.

The maximum allowed temperature ($T_{\max}$) inside the reactor was chosen 10 degrees smaller than the real limit (400 K) in order to give to the feedback controller enough room of maneuverability. The trade-off coefficient w was found by means of a trial and error process and the local input constraint $T_J^{\Delta_{max}}$ was selected in such a way that the differences between the non-linear and linear model are small.

The algorithm was executed using different initial conditions and some of the results obtained are presented in table II. Along the experiments, three local minima were found, however it does not mean that these are the only ones. This was an expected result due to the nature of the optimization problem. These local minima could be unified by modifying the cost function, for instance, by adding a term that punishes the temperature deviation at the reactor output.

The selection of the optimal temperature and concentration profiles was done by checking the value of the cost function and the deviation of the temperature at the reactor output with respect to the temperature of the feeding flow. In many practical situations, a large deviation is undesirable since it increases the heat loss [3].

From the three local minima, the second one ($T_{J1} = 374.6$ K, $T_{J2} = 310.1$ K and $T_{J3} = 325.2$ K) was chosen since it had the smallest value for the cost function and a small temperature deviation at the reactor output. The optimal concentration and temperature profiles can be observed in figure

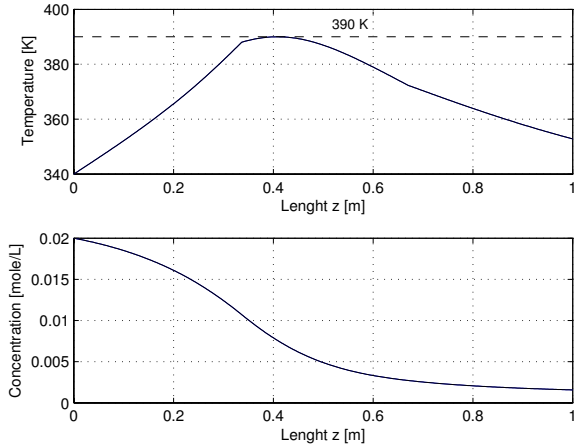

Fig. 2. Steady-State Concentration and Temperature profiles (Operating Profiles) when $T_{J1} = 374.6$ K, $T_{J2} = 310.1$ K and $T_{J3} = 325.2$ K.

2. The concentration at the reactor output is $1.5737 \cdot 10^{-3}$ mole/L which is 12.7 times smaller than the concentration of the feeding flow (0.02 mole/L). In addition, the maximum peak of the temperature inside the reactor is 390 K, satisfying in this way the temperature constraint.

B. Linear Model

By using the Taylor Series, the linear model of the tubular chemical reactor was obtained after linearizing (1) around the jackets temperatures and the operating profiles shown in figure 2. This linear model is as follows:

$$\begin{aligned} \frac{\partial C^{\Delta}}{\partial t} &= -v\frac{\partial C^{\Delta}}{\partial z} - \alpha_A C^{\Delta} - \alpha_B T^{\Delta} \\ \frac{\partial T^{\Delta}}{\partial t} &= -v\frac{\partial T^{\Delta}}{\partial z} - \alpha_C C^{\Delta} - \alpha_D T^{\Delta} + H_r T_w^{\Delta} \end{aligned} \tag{6}$$

with the following boundary conditions (tubular reactor with closed ends):

$$C^{\Delta} = C_{in} - C_{in}^*, \quad T^{\Delta} = T_{in} - T_{in}^* \text{ at } z = 0$$

where

$$\alpha_A(z) = k_0 e^{-\frac{E}{RT^*}}, \ \alpha_B(z) = k_0 C^* \frac{E}{RT^{*2}} e^{-\frac{E}{RT^*}}$$

$$\alpha_C(z) = -G_r e^{-\frac{E}{RT^*}}, \ \alpha_D(z) = -G_r C^* \frac{E}{RT^{*2}} e^{-\frac{E}{RT^*}} + H_r$$

C^*, T^*, T_w^* are the steady state profiles (operating profiles) of the concentration, temperature and reactor wall temperature respectively, C_{in}^* and T_{in}^* are the concentration and temperature in steady state of the feeding flow, $C^{\Delta} = C - C^*$, $T^{\Delta} = T - T^*$, $T_w^{\Delta} = T_w - T_w^*$ are the deviations from steady state of the concentration, temperature and reactor wall temperature.

In order to reduce the infinite dimensionality of (6), the partial derivatives with respect to space are replaced by backward difference approximations resulting in a system of ODEs as follows:

$$\begin{aligned} \frac{d\bar{C}_i^{\Delta}}{dt} &= -\frac{v}{\Delta z}\left(\bar{C}_i^{\Delta} - \bar{C}_{i-1}^{\Delta}\right) - \alpha_{A,i}\bar{C}_i^{\Delta} - \alpha_{B,i}\frac{T_f}{C_f}\bar{T}_i^{\Delta} \\ \frac{d\bar{T}_i^{\Delta}}{dt} &= -\frac{v}{\Delta z}\left(\bar{T}_i^{\Delta} - \bar{T}_{i-1}^{\Delta}\right) - \alpha_{C,i}\frac{C_f}{T_f}\bar{C}_i^{\Delta} - \alpha_{D,i}\bar{T}_i^{\Delta} + H_r\bar{T}_{w,i}^{\Delta} \end{aligned} \tag{7}$$

with,

$$\bar{C}_0^{\Delta} = \bar{C}_{in}^{\Delta}, \ \bar{T}_0^{\Delta} = \bar{T}_{in}^{\Delta}$$

$$for \ i = 1, 2, .., N$$

where $\alpha_{A,i} = \alpha_A(z_i)$, $\alpha_{B,i} = \alpha_B(z_i)$, $\alpha_{C,i} = \alpha_C(z_i)$, $\alpha_{D,i} = \alpha_D(z_i)$, $z_i = i \cdot \Delta z$, $C_i^*, T_i^*, T_{w,i}^*$ are the steady state concentration, temperature and reactor wall temperature of the i-th section, $\bar{C}_i^{\Delta} = (C_i - C_i^*)/C_f$, $\bar{T}_i^{\Delta} = (T_i - T_i^*)/T_f$, $\bar{T}_{w,i}^{\Delta} = (T_{w,i} - T_{w,i}^*)/T_f$ are the normalized deviations from steady state of the concentration, temperature and reactor wall temperature of the i-th section, $\bar{C}_{in}^{\Delta} = (C_{in} - C_{in}^*)/C_f$ and $\bar{T}_{in}^{\Delta} = (T_{in} - T_{in}^*)/T_f$ are the normalized deviations from steady state of the concentration and temperature of the feeding flow, N is the number of sections in which the reactor is divided, T_f and C_f are normalization factors, and Δz is the length of each section.

If we define the following vectors,

$$\mathbf{x}(t) = (\bar{C}_1^{\Delta}, \bar{C}_2^{\Delta}, ..., \bar{C}_N^{\Delta}, \bar{T}_1^{\Delta}, \bar{T}_2^{\Delta}, ..., \bar{T}_N^{\Delta})^T$$

$$\mathbf{d}(t) = (\bar{C}_{in}^{\Delta}, \bar{T}_{in}^{\Delta})^T$$

$$\mathbf{u}(t) = (\bar{T}_{J1}^{\Delta}, \bar{T}_{J2}^{\Delta}, \bar{T}_{J3}^{\Delta})^T$$

then (7) can be cast as follows:

$$\dot{\mathbf{x}}(t) = \mathbf{A}\mathbf{x}(t) + \mathbf{B}\mathbf{u}(t) + \mathbf{F}\mathbf{d}(t) \tag{8}$$

where $\mathbf{A}$, $\mathbf{B}$ and $\mathbf{F}$ are the matrices describing the system, $\mathbf{u}(t)$ is the vector of the inputs and $\mathbf{d}(t)$ is the vector of the disturbances.

The spatial domain was divided into $N = 300$ sections which means that the system has 600 states. Since it is not easy to design a control system that can deal with 600 states, a reduced order model must be found. In this paper such reduced order model is derived by means of a POD approach.

III. Model Reduction using POD

In proper orthogonal decomposition, we postulate that $\mathbf{x}(t) \in \Re^{2N}$ can be expanded as a sum of orthonormal basis functions (or spectral form):

$$\mathbf{x}(t) = \sum_{j=1}^{2N} a_j(t)\varphi_j(z_d) \tag{9}$$

$$\varphi_j(z_d) \in \Re^{2N}, \ \ a_j(t) \in \Re$$

where $\{\varphi_j(z_d)\}_{j=1}^{2N}$ is a set of orthonormal basis functions (POD basis functions) in the discretized spatial domain z_d, and $\{a_j(t)\}_{j=1}^{2N}$ are the time varying coefficients or POD coefficients associated to each basis function. These POD basis functions are ordered according to their relevance to $\mathbf{x}$(t).

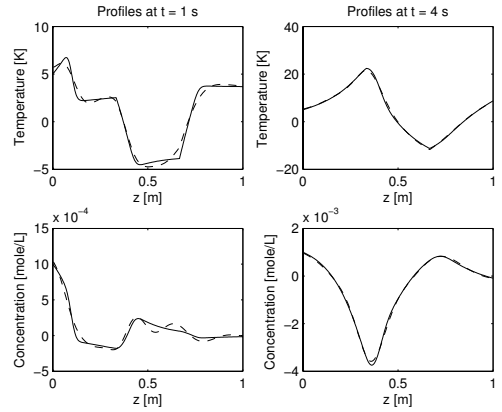

Fig. 3. Temperature and Concentration deviation profiles at $t = 1s$ and $t = 4s$. Solid line - full order Model. Dashed line - reduced order model.

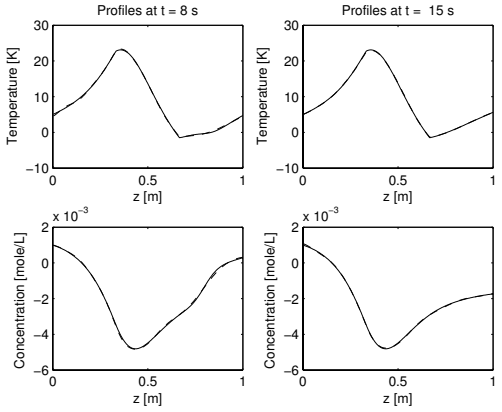

Fig. 4. Temperature and Concentration deviation profiles at $t = 8s$ and $t = 15s$. Solid line - full order Model. Dashed line - reduced order model.

The main dynamics of the system can be represented using the first n most relevant basis functions, since $\{\varphi_j(z_d)\}_{j=1}^{n}$ condensates the main spatial correlations. An n-th order approximation of (9) is then given by means of the truncated sequence

$$\mathbf{x}_n(t) = \sum_{j=1}^{n} a_j(t)\varphi_j(z_d), \quad n << 2N. \tag{10}$$

An approximate (reduced order) model of $\mathbf{x}(t)$ can be derived by building a model for the first n time varying coefficients. "This is the essence of model reduction by POD".

The POD basis Functions are determined from simulation or experimental data (Snapshot matrix) of the process. The dynamic model for the first n time varying coefficients can be found by means of the Galerkin projection [4] or using subspace identification techniques [5].

The derivation of a reduced order model of (8) was done in 5 steps. These steps are described in the following subsections.

A. Generation of the snapshot Matrix

A snapshot matrix $\mathbf{X}_{snap} \in \Re^{600\times1500}$ was constructed from the system response when independent step changes were made in the input ($\mathbf{u}(t)$) and perturbation ($\mathbf{d}(t)$) signals of the linear model (8).

$$\mathbf{X}_{snap} = (\mathbf{x}(t = \Delta t), \ldots, \mathbf{x}(t = 1500\Delta t)) \tag{11}$$

Along the simulations, 1500 samples were collected using a sampling time (Δt) of 0.05 sec. The amplitude of the step changes were chosen in such a way that each one produces changes of similar magnitude in the temperature and concentration profiles.

B. Derivation of the POD Basis Functions

They were derived by calculating the singular value decomposition (SVD) of $\mathbf{X}_{snap}$,

$$\mathbf{X}_{snap} = \mathbf{\Phi}\mathbf{\Sigma}\mathbf{\Psi}^T$$

where $\mathbf{\Phi} \in \Re^{600\times600}$ and $\mathbf{\Psi} \in \Re^{1500\times1500}$ are unitary matrices, and $\mathbf{\Sigma} \in \Re^{600\times1500}$ is a matrix which contains the singular values of $\mathbf{X}_{snap}$ in a decreasing order on its main diagonal.

The columns of Φ are the POD basis functions.

$$\mathbf{\Phi} \in \Re^{600\times600} = (\varphi_1, \varphi_2, \ldots \varphi_{600})$$

C. Selection of the most relevant POD basis functions

It was done by checking the singular values of $\mathbf{X}_{snap}$. The larger the singular value the more relevant the basis function is.

The first 20 basis functions associated to the first 20 largest singular values were selected. The 20th order approximation of $\mathbf{x}(t)$ is given by

$$\mathbf{x}_n(t) = \sum_{j=1}^{20} a_j(t)\varphi_j(z_d) = \mathbf{\Phi}_n\mathbf{a}(t) \tag{12}$$

where $\mathbf{\Phi}_n = (\varphi_1, \varphi_2, \ldots \varphi_{20})$ and $\mathbf{a}(t) = (a_1(t), a_2(t), \ldots, a_{20}(t))^T$.

D. Construction of the model for the first n=20 POD coefficients

In order to derive the model for the POD coefficients the Galerkin projection was used. If we define a residual function $R(\mathbf{x})$ for equation (8) as follows:

$$R(\mathbf{x}) = \dot{\mathbf{x}}(t) - \mathbf{A}\mathbf{x}(t) - \mathbf{B}\mathbf{u}(t) - \mathbf{F}\mathbf{d}(t) \tag{13}$$

and we replace $\mathbf{x}(t)$ by its n-th order approximation $\mathbf{x}_n(t)$ in (13), the Galerkin projection states that the projection of $R(\mathbf{x}_n)$ on the space spanned by the basis functions $\mathbf{\Phi}_n$ vanishes. That is,

$$\langle R(\mathbf{x}_n), \varphi_j(z_d)\rangle = 0; \quad j = 1, \ldots n \tag{14}$$

where $\langle .,. \rangle$ denotes inner product. Replacing $\mathbf{x}(t)$ by its n-th order approximation $\mathbf{x}_n(t) = \mathbf{\Phi}_n\mathbf{a}(t)$ in equation (8), and applying the inner product criterion (Galerkin projection) to the resulting equation we have:

$$\langle \mathbf{\Phi}_n\dot{\mathbf{a}}(t), \mathbf{\Phi}_n\rangle = \langle \mathbf{A}\mathbf{\Phi}_n\mathbf{a}(t) + \mathbf{B}\mathbf{u}(t) + \mathbf{F}\mathbf{d}(t), \mathbf{\Phi}_n\rangle\,. \tag{15}$$

By evaluating the inner product in (15),

$$\mathbf{\Phi}_n^T\mathbf{\Phi}_n\dot{\mathbf{a}}(t) = \mathbf{\Phi}_n^T\mathbf{A}\mathbf{\Phi}_n\mathbf{a}(t) + \mathbf{\Phi}_n^T\mathbf{B}\mathbf{u}(t) + \mathbf{\Phi}_n^T\mathbf{F}\mathbf{d}(t)$$

$$\dot{\mathbf{a}}(t) = \mathbf{\Phi}_n^T\mathbf{A}\mathbf{\Phi}_n\mathbf{a}(t) + \mathbf{\Phi}_n^T\mathbf{B}\mathbf{u}(t) + \mathbf{\Phi}_n^T\mathbf{F}\mathbf{d}(t) \qquad (16)$$

we obtain the model for the first n time varying coefficients. Finally, the reduced order model of the reactor with only 20 states is,

$$\dot{\mathbf{a}}(t) = \mathbf{A}_r\mathbf{a}(t) + \mathbf{B}_r\mathbf{u}(t) + \mathbf{F}_r\mathbf{d}(t) \qquad (17)$$

$$\mathbf{x}_n(t) = \mathbf{\Phi}_n\mathbf{a}(t)$$

where $\mathbf{A}_r = \mathbf{\Phi}_n^T\mathbf{A}\mathbf{\Phi}_n$, $\mathbf{B}_r = \mathbf{\Phi}_n^T\mathbf{B}$ and $\mathbf{F}_r = \mathbf{\Phi}_n^T\mathbf{F}$.

E. Validation of the reduced order model

For validating the reduced order model, constant input signals $\bar{T}_{J1}^{\Delta}(t) = 0.0294$ ($T_{J1}^{\Delta}(t) = 10$ K), $\bar{T}_{J2}^{\Delta}(t) = -0.0588$ ($T_{J2}^{\Delta}(t) = -20$ K) and $\bar{T}_{J3}^{\Delta}(t) = 0.0588$ ($T_{J3}^{\Delta}(t) = 20$ K) and constant perturbation signals $\bar{C}_{in}^{\Delta}(t) = 0.05$ ($C_{in}^{\Delta}(t) = 10^{-3}$ mole/L) and $\bar{T}_{in}^{\Delta}(t) = 0.0147$ ($T_{in}^{\Delta}(t) = 5$ K) were applied to the full order model and to the reduced order model, and afterwards their outputs were compared. Figures 3 and 4 show the temperature and concentration deviation profiles of the reactor at different time instants for each model. During the first seconds we can appreciate some differences between the models, but as the simulation advances, these differences become negligible and really difficult to observe. In order to measure the quality of the reduced order model the averages of the absolute error for the temperature and concentration were calculated by means of the following formulas:

$$\varepsilon_T = \frac{T_f}{N_s}\sum_{k=1}^{N_s}\left|\bar{\mathbf{T}}^{\Delta}(k\Delta t) - \bar{\mathbf{T}}_n^{\Delta}(k\Delta t)\right|$$

$$\varepsilon_C = \frac{C_f}{N_s}\sum_{k=1}^{N_s}\left|\bar{\mathbf{C}}^{\Delta}(k\Delta t) - \bar{\mathbf{C}}_n^{\Delta}(k\Delta t)\right|$$

where $N_s = 300$ is the number of time steps and $\Delta t = 0.05s$. For the temperature profile, the maximum value for the error (ε_T) was 0.405 Kelvin. For the concentration, the maximum peak for the error (ε_C) was $9.35 \cdot 10^{-5}$ mole/L. From the previous results we can conclude that the reduced order model with only 20 states provides an acceptable approximation of the full order model (600 states). The discrete-time version of (17) that is used for designing the digital controller, was obtained using the discretization method known as zero-order hold with a sampling time of $0.2s$,

$$\mathbf{a}(k+1) = \tilde{\mathbf{A}}\mathbf{a}(k) + \tilde{\mathbf{B}}\mathbf{u}(k) + \tilde{\mathbf{F}}\mathbf{d}(k) \qquad (18)$$

$$\mathbf{x}_n(k) = \mathbf{\Phi}_n\mathbf{a}(k)$$

where $\tilde{\mathbf{A}}$, $\tilde{\mathbf{B}}$ and $\tilde{\mathbf{F}}$ are the matrices describing the new system. The sampling time was chosen by dividing the faster time constant (it was determined through step tests) of (17) by 10.

IV. Control System

The control goal is to reject the disturbances that affect the reactor, that is the changes in the temperature and concentration of the feeding flow. The control actions must satisfy the input constraints of the process (280 K$\leq T_{J1}(t) \leq$ 400 K, 280 K$\leq T_{J2}(t) \leq$ 400 K and 280 K$\leq T_{J3}(t) \leq$ 400 K). In addition, the control system must keep the temperature inside the reactor below 400 K. Since the control system has to keep the reactor operating around the profiles shown in figure 2, the reference ($\mathbf{x}_{ref}$) for the vector $\mathbf{x(t)}$ is $\mathbf{0}$. Furthermore, given that $\mathbf{x}_{ref}$ can be expressed in terms of the POD coefficients as follows:

$$\mathbf{r} = \mathbf{\Phi}^T\mathbf{x}_{ref} \qquad (19)$$

we can control the temperature and concentration profiles of the reactor by controlling the POD coefficients. The reference vector for the first 20 POD coefficients is denoted by $\mathbf{a}_{ref}$ and is equal to the first 20 elements of the vector $\mathbf{r}$ in (19). For controlling these POD coefficients and consequently the temperature and concentration profiles of the reactor, an MPC controller with a disturbance model was designed. In this scheme the MPC controller uses the reduced order model given by (18) to predict the future behavior of the process.

The formulation of the MPC controller with a disturbance model is given by

$$\min_{a,\Delta u} J = \sum_{k=1}^{N_p}\left(\mathbf{a}_{ref}(k) - \mathbf{a}(k)\right)^T\mathbf{Q}\left(\mathbf{a}_{ref}(k) - \mathbf{a}(k)\right) + \sum_{k=0}^{Nc-1}\mathbf{\Delta u}(k)^T\mathbf{R}\mathbf{\Delta u}(k) \qquad (20)$$

subject to

$$\mathbf{a}(k+1) = \tilde{\mathbf{A}}\mathbf{a}(k) + \tilde{\mathbf{B}}\mathbf{u}(k) + \tilde{\mathbf{F}}\mathbf{d}(k)$$
$$\mathbf{d}(k+1) = \mathbf{d}(k)$$
$$\mathbf{u}_{\min} \leq \mathbf{u}(k) \leq \mathbf{u}_{\max}$$

where $\Delta\mathbf{u}(k) = \mathbf{u}(k) - \mathbf{u}(k-1)$, N_p is the prediction horizon, N_c is the control horizon, $\mathbf{Q}$ and $\mathbf{R}$ are weighting matrices, and $\mathbf{u}_{min}$ and $\mathbf{u}_{max}$ are the lower and upper bounds of $\mathbf{u}(k)$.

It is important to remember that in this process only the disturbance related to the changes in the temperature of the feeding flow is measured directly. The changes in the concentration of the feeding flow are not measured. Since the first element ($d_1(k) = \bar{C}_{in}^{\Delta}(k)$) of the disturbance vector $\mathbf{d}(k)$ is unknown, and the state vector $\mathbf{a}(k)$ is also unknown, they were estimated by means of an observer (in this case a Kalman Filter) with the following formulation:

$$\begin{pmatrix} \hat{\mathbf{a}}(k+1) \\ \hat{d}_1(k+1) \end{pmatrix} = \begin{pmatrix} \tilde{\mathbf{A}} & \tilde{\mathbf{F}}_C \\ \mathbf{0} & 1 \end{pmatrix}\begin{pmatrix} \hat{\mathbf{a}}(k) \\ \hat{d}_1(k) \end{pmatrix} + \begin{pmatrix} \tilde{\mathbf{B}} \\ \mathbf{0} \end{pmatrix}\mathbf{u}(k) + \begin{pmatrix} \tilde{\mathbf{F}}_T \\ 0 \end{pmatrix}d_2(k) + \begin{pmatrix} \mathbf{L}_a \\ \mathbf{L}_d \end{pmatrix}\left(\mathbf{y}(k) - \hat{\mathbf{y}}(k)\right) \qquad (21)$$

$$\hat{\mathbf{y}}(k) = \mathbf{C}_s\hat{\mathbf{x}}_n(k) = \mathbf{C}_s\mathbf{\Phi}_n\hat{\mathbf{a}}(k)$$

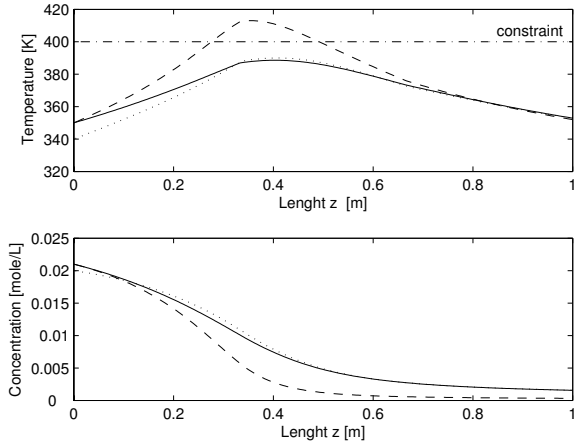

Fig. 5. Steady-State Temperature and Concentration profiles for test 1. Dotted line - reference. Dashed line - open loop response. Solid Line - MPC controller.

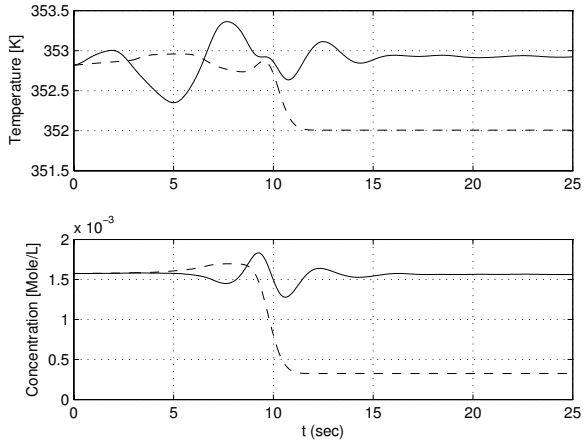

Fig. 6. Temperature and concentration at the reactor output during test 1. Dashed line - open loop response. Solid Line - MPC controller.

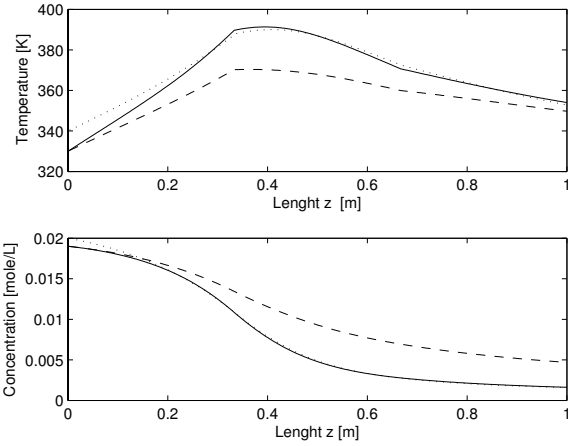

Fig. 7. Steady-State Temperature and Concentration profiles for test 2. Dotted line - reference. Dashed line - open loop response. Solid Line - MPC controller.

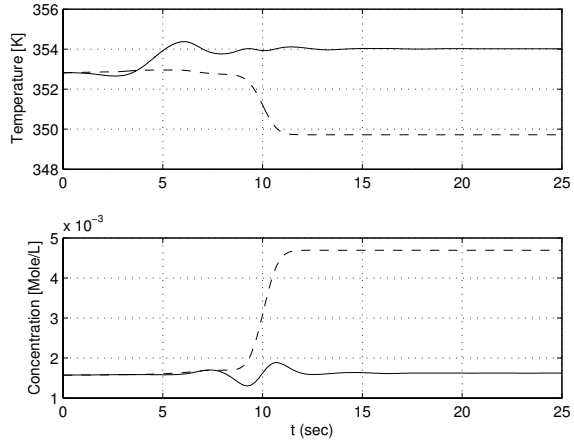

Fig. 8. Temperature and concentration at the reactor output during test 2. Dashed line - open loop response. Solid Line - MPC controller.

where $\hat{\mathbf{a}}(k)$ is the estimated vector of the POD coefficients, $\hat{d}_1(k)$ is the estimation of $\bar{C}_{in}^{\Delta}(k)$, $d_2(k)$ is the normalized temperature deviations of the feeding flow ($\bar{T}_{in}^{\Delta}(k)$), $\mathbf{y}(k) \in \Re^4$ is a vector which contains the temperature measurements (normalized deviations) along the reactor, $\hat{\mathbf{y}}(k)$ is the estimation of $\mathbf{y}(k)$, $\mathbf{L}_a$ and $\mathbf{L}_d$ are the submatrices of the observer gain (Kalman gain), $\tilde{\mathbf{F}}_C$ and $\tilde{\mathbf{F}}_T$ are the column vectors of $\tilde{\mathbf{F}} = (\tilde{\mathbf{F}}_C, \tilde{\mathbf{F}}_T)$ and $\mathbf{C}_s$ is a selection matrix which selects the measured temperatures from the vector $\mathbf{x}_n(k)$.

The control horizon N_c was set to 10 samples and the prediction horizon N_p was selected according to the following criterion: "Prediction Horizon = Control Horizon + Largest Settling Time = 80 samples". $\mathbf{u}_{min}$ and $\mathbf{u}_{max}$ were selected according to the input constraints of the process and the operating temperatures of the jackets, and the weighting matrices in this way: $\mathbf{Q} = \mathbf{I}_{20\times 20}$, $\mathbf{R} = 110 \cdot \mathbf{I}_{3\times 3}$.

In order to evaluate the performance of the control system, the following tests were carried out:

- Test 1: in this test the temperature of the feeding flow is increased in 10 K and the concentration of the feeding flow is increased in 10^{-3} mole/L. This test has a big impact on the temperature profile of the reactor.
- Test 2: in this test the temperature and concentration of the feeding flow are decreased in 10 K and 10^{-3} mole/L respectively. This test has a big impact on the concentration profile of the tubular reactor.

For the simulations, the nonlinear model of the process given in (1) was discretized in space by replacing the partial derivatives with respect to space by backward difference approximations [1][7].

The simulation results of the test 1 are presented in figures 5 and 6. Figures 7 and 8 show the simulation results of the test 2. Furthermore, some quantities of interest are given in table III. In this table, T_{max} is the maximum temperature reached inside the reactor during the test. ΔC_{out} is the percentage of change of the concentration in steady state

TABLE III
SOME QUANTITIES EXTRACTED FROM THE TESTS

Control	Test 1		Test 2	
	T_{max} [K]	$\Delta C_{out}[\%]$	T_{max} [K]	$\Delta C_{out}[\%]$
Open-Loop	413.03	-79.39	390	198.25
MPC	394.09	-0.69	397.59	3.19

at the reactor output with respect to its nominal value. That is,

$$\Delta C_{out}(\%) = \frac{C_N - C_N^*}{C_N^*} \times 100$$

where C_N^* is the nominal value ($1.5737 \cdot 10^{-3}$ mole/L) and C_N is the concentration in steady state after the test.

In the test 1 for the open-loop case, the increment in the temperature and concentration of the feeding flow increases the temperature inside the reactor in such a way that the temperature constraint is violated (see figure 5), both in transient time and in steady state. The maximum temperature value registered was 413.03 K, which is far from the maximum temperature allowed (400 K). The concentration (steady state) at the reactor output is reduced in 79.39 % as a consequence of the increment of the temperature inside the reactor beyond the allowed limit. On the other hand, the MPC controller keeps the temperature inside the reactor below 400 K and at the same time it reduces a little bit the concentration at the reactor output. Although it is not shown in this paper, the control efforts of the MPC controller were all the time within the boundaries.

In the test 2, the decrement in the temperature and concentration of the feeding flow increases significantly the concentration at the reactor output when the system is operating in an open-loop configuration (see figures 7 and 8). We have an increment of 198.25% in steady state, which means that the performance of the tubular chemical reactor has been reduced dramatically. The MPC overcomes this situation by manipulating the temperatures of the jackets in such a way that the temperature inside the reactor is increased in order to compensate the effect of the input disturbances. With the MPC controller we have an increment in the concentration (steady-state) of only 3.19%, which is 62.14 times smaller than in the open-loop case. It is important to remark that the temperature inside the reactor (maximum value = 397.59 K) satisfied the temperature constraint along the simulation. Additionally, the control actions were all the time within the limits.

From the previous tests we can conclude that the MPC controller based on the POD model of the process showed a good behavior for rejecting the disturbances that affect the reactor.

V. CONCLUSIONS

In this paper the results of applying POD and Predictive control techniques to the control of the temperature and concentration profiles of a non-isothermal tubular reactor have been presented. Additionally, an optimization algorithm has been described for deriving the optimal operating profiles of the process. A significant model reduction has been achieved by means of the POD technique that has made possible the control design.

In spite of the spatial discretization of the nonlinear PDEs that model the reactor, the linearization and discretization in time of the equations, and the dramatic reduction of model order by means of POD, on which the controller is based, the controller performed well. However, if larger disturbances are applied to the tubular chemical reactor, the behavior of the MPC controller would not be as good as it has been thus far, since the differences between the nonlinear model and the linear model and consequently the reduced order model would be more significant. Therefore in future work, the nonlinear characteristics of the process should be taken into account in order to design controllers with a higher degree of robustness.

VI. ACKNOWLEDGMENTS

This research was supported by: • Research Council KUL: GOA AMBioRICS, CoE EF/05/006 Optimization in Engineering, several PhD/postdoc & fellow grants; • Flemish Government: ○ FWO: PhD/postdoc grants, projects, G.0407.02 (support vector machines), G.0197.02 (power islands), G.0141.03 (Identification and cryptography), G.0491.03 (control for intensive care glycemia), G.0120.03 (QIT), G.0452.04 (new quantum algorithms), G.0499.04 (Statistics), G.0211.05 (Nonlinear), G.0226.06 (cooperative systems and optimization), G.0321.06 (Tensors), G.0302.07 (SVM/Kernel), research communities (ICCoS, ANMMM, MLDM); ○IWT: PhD Grants, McKnow-E, Eureka-Flite2; • Belgian Federal Science Policy Office: IUAP P6/04 (Dynamical systems, control and optimization, 2007-2011) ; • EU: ERNSI. Dr. Bart De Moor is a full professor at the Katholieke Universiteit Leuven, Belgium.

REFERENCES

[1] I.Y. Smets, J.F. Van Impe,"Optimal Control of Tubular Chemical Reactors: Performance Assessment under transient and Diffuse conditions", *in Proceedings of the 10th Mediterranean Conference on Control and Automation - MED2002*, Lisbon, Portugal, 2002.

[2] M. Fjeld and B. Ursin, "Approximate lumped models of a tubular chemical reactor, and their use in feedback and feedforward control", *in Proceedings of the 2nd IFAC Symposium on Multivariable Technical Control Systems*, pp. 1-18, North Holland, Amsterdam, 1971.

[3] I.Y. Smets, D. Dochain and J.F. Van Impe, Optimal Temperature control of a steady-state exothermic Plug-flow Reactor, *AIChE Journal*, vol. 48 (2), pp. 279-286, 2002.

[4] P. Astrid, "Reduction of Process Simulation Models: a proper orthogonal decomposition approach", Ph.D. thesis, Technishche Universiteit Eindhoven, Eindhoven, Netherlands, 2004.

[5] L. Huisman,"Control of Glass Melting Processes Based on Reduced CFD models", Ph.D. thesis, Technishche Universiteit Eindhoven, Eindhoven, Netherlands, 2005.

[6] M. Hazenberg, P. Astrid and S. Weiland, "Low order modeling and optimal control design of a heated plate", *in Proceedings of the 5th European Control Conference*, Cambridge, 2003.

[7] D. Del Vecchio and N. Petit, "Boundary Control for an industrial under-actuated tubular chemical reactor", *Journal of Process Control*, vol 15, pp. 771-784, 2005